Assembly Conditions of Parallel Manipulators Considering Geometric Errors, Joint Clearances, Link Flexibility and Joint Elasticity

Davide Corradi, Stéphane Caro, Damien Chablat, Philippe Cardou

Assembly Conditions of Parallel Manipulators Considering Geometric Errors, Joint Clearances, Link Flexibility and Joint Elasticity

Davide Corradi[1], Stéphane Caro[2], Damien Chablat[2] and Philippe Cardou[3]

***Abstract*— This paper presents a methodology to analyze the assembly conditions of parallel manipulators and compute the maximum pose errors of their moving platform, while considering geometric errors, joint clearances, link flexibility and joint elasticity. First, the proposed methodology consists in determining the zone(s) of the manipulator workspace in which the manipulator can be assembled assuming that its links and joints are rigid, while taking into account geometric errors and joint clearances. Then, the minimum energy required to assemble the manipulator in the non-assembly zone(s) is computed, while considering link flexibility and joint elasticity. The maximum pose errors of the moving-platform are also computed throughout the manipulator workspace. Finally, a two-dof spatial parallel manipulator, named IRSbot-2, is used as an illustrative example.**

I. Introduction

Accuracy is one of the key features that favor robotic manipulators for many industrial applications. Superior levels of accuracy are achieved by controlling or measuring all possible sources of errors on the pose of the moving platform of a robotic manipulator. Among the most important sources of errors, we find manufacturing errors, assembly errors, compliance in the mechanical architecture, resolution of the servoactuators, backlash in the reductors, and clearances in the joints. Parallel manipulators are usually assumed to be more accurate than their serial counterparts. However, this accuracy can be affected by the joint clearances required for the assembly of the manipulators. The focus of this paper is the impact of geometric errors, joint clearances, link flexibility and joint elasticity on the assembly conditions of parallel manipulators and on the maximum pose errors of their moving platform.

Geometric errors are caused by the imperfect fabrication and assembly of the elements of the robot. Their effect on accuracy is usually measurable and repeatable, and can therefore be compensated through appropriate calibration.

The relative motions of the two parts of a *joint* with *clearance* may cause undesirable effects such as moving-platform pose errors [1], [2], [3], [4], [5], impacts, wear, vibrations and noise [6], [7]. Their influence on the behaviour of the manipulator is not repeatable and therefore difficult to model and to calibrate, and reducing them usually leads to high manufacturing costs.

If the stiffness of the links and of the joints is not sufficient, their deformation will be able to cause a notable effect on the accuracy of the manipulator, especially when subjected to heavy loads or at high speeds [8], [9], [10]. The Virtual Joint Model (VJM) approach is convenient to deal with *link flexibility* and *joint elasticity* in robotic manipulators [11], [12], [13].

This paper introduces a methodology to analyse the assembly conditions of parallel manipulators and compute the maximum pose errors of their moving platform, while considering geometric errors, joint clearances, link flexibility and joint elasticity. First, the proposed methodology consists in determining the zone(s) of the manipulator workspace in which the manipulator can be assembled assuming that its links and joints are rigid, while taking into account geometric errors and joint clearances. Then, the minimum energy required to assemble the manipulator in the non-assembly zone(s) is computed, while considering link flexibility and joint elasticity. The maximum pose errors of the moving-platform are also computed throughout the manipulator workspace. By applying the method for different sets of parameters (clearances, maximum geometric errors, stiffness of joints and links) it is possible to choose the best option with regard to accuracy and internal deformations.

The novelty of this method resides in the fact that many sources of inaccuracies are considered at the same time, and in the fact that it provides not only an estimate of the pose error, but also of the internal forces of the manipulator in different configurations. Existing studies mainly focus on one element (joint clearances, geometric errors, or flexibilities) and provide methods only for accuracy analysis or force analysis.

Section II deals with the modeling of geometric errors, joint clearances, link flexibility and joint elasticity. Section III describes the method used to compute the assembly zones, the minimum assembly energy, the reaction wrench on the moving-platform and the maximum pose errors of the moving-platform throughout the manipulator workspace. Section IV provides an illustrative example in order to highlight the contributions of the paper.

*This work was partially supported by the Agence Nationale de la Recherche (ANR), France (Project ANR-2011-BS3-006-01-ARROW).

[1]D. Corradi is with Ecole Centrale de Nantes, Nantes, France, and with the Interdisciplinary Center for Scientific Computing (IWR), Heidelberg University, Heidelberg, Germany davide.corradi@iwr.uni-heidelberg.de

[2]S. Caro and D. Chablat are with CNRS–IRCCyN, Nantes, France stephane.caro@irccyn.ec-nantes.fr, damien.chablat@irccyn.ec-nantes.fr

[3]P. Cardou is with Robotics Laboratory, Department of Mechanical Engineering, Université Laval, Quebec, Canada pcardou@gmc.ulaval.ca

II. Modeling geometric errors, joint clearances and flexibilities

A. Frame Conventions and Nomenclature

Parallel manipulators with m legs are considered. Each leg comprises n_i joints and B_i loops. A fixed base frame $\mathcal{F}_0$, common to all the legs, is arbitrarily defined. A frame $\mathcal{F}_p$ is attached to the moving-platform of the manipulator. All the other frames, attached to the joints and the end effectors of the legs, are denoted $\mathcal{F}_{i,j}$, $j = 1 \dots N_i$. Each frame has only one antecedent frame, whose index is denoted as $ant(i,j)$. When $\mathcal{F}_{i,j}$ is attached to a joint, it is defined according to the Denavit-Hartenberg convention: axis $\mathbf{z}_{i,j}$ is along the axis of the joint, and axis $\mathbf{x}_{i,j}$ is along the common normal to axes $\mathbf{z}_{ant(i,j)}$ and $\mathbf{z}_{i,j}$. The frame attached to the end-effector of leg i is denoted $\mathcal{F}_{i,e}$. When the manipulator is assembled, the frames attached to the end-effectors of the legs coincide with the frame attached to the platform, so that $\mathcal{F}_{i,e} \equiv \mathcal{F}_p, i = 1 \dots m$. Each loop is cut at a passive joint, and the frames that are attached to the two cut ends of the k-th loop of leg i are denoted $\mathcal{F}_{i,k_a}$ and $\mathcal{F}_{i,k_b}$. These two frames should coincide once the manipulator is assembled, i.e., $\mathcal{F}_{i,k_a} \equiv \mathcal{F}_{i,k_b}$. The transformation matrix from $\mathcal{F}_{ant(i,j)}$ to $\mathcal{F}_{i,j}$ is denoted $\mathbf{T}_{i,j}$, while the corresponding rotation matrix and translation vector are denoted $\mathbf{R}_{i,j}$ and $\mathbf{t}_{i,j}$, respectively.

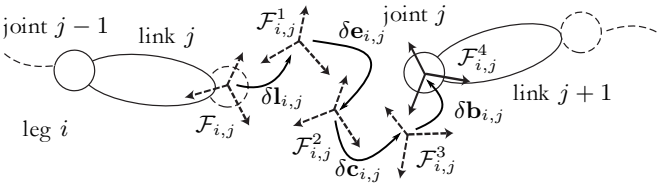

Fig. 1. Effect of geometric errors, link flexibility, joint clearances and joint elasticity on the pose of frame $\mathcal{F}_{i,j}$. $\mathcal{F}_{i,j}$ is moved to $\mathcal{F}^1_{i,j}$ by geometric errors, to $\mathcal{F}^2_{i,j}$ by link elasticity, to $\mathcal{F}^3_{i,j}$ by clearances and finally to $\mathcal{F}^4_{i,j}$ by joint elasticity.

B. Geometric Errors

The geometric errors of the jth link of leg i are supposed to be small and measurable. They are represented by the small displacement screw $\delta\mathbf{l}_{i,j}$ as shown in Fig. 1.

C. Joint Clearances

Intuitively, clearances in a joint are best modeled by bounding its associated errors below and above. Clearances in the jth joint of leg i are represented by the small displacement screw $\delta\mathbf{c}_{i,j}$ as shown in Fig. 1. Assuming that the lower and upper bounds are the same, this generally yields six parameters that bound the error screw $\delta\mathbf{c}_{i,j}$. In the case of a revolute joint, however, we can take advantage of the axisymmetry to reduce the number of parameters to four, grouped in vector $\bar{\mathbf{c}}_{i,j}$. The elements of $\delta\mathbf{c}_{i,j}$ and of

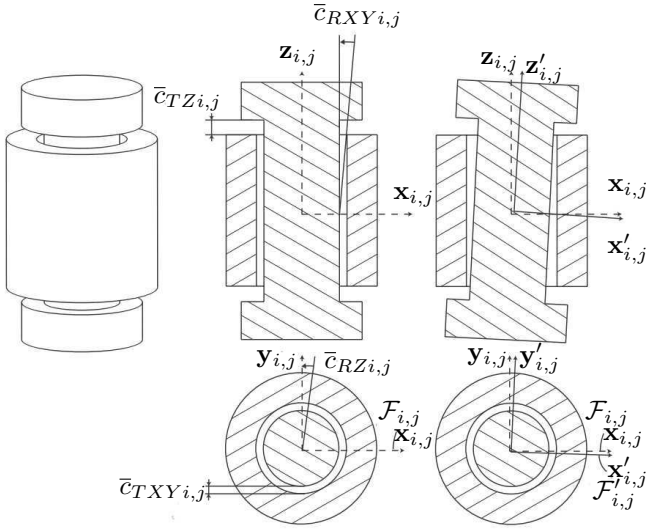

Fig. 2. Axisymmetric revolute joint with clearance. Clearance causes a displacement that transforms frame $\mathcal{F}_{i,j}$ to frame $\mathcal{F}'_{i,j}$.

$\bar{\mathbf{c}}_{i,j}$ are denoted as follows (see Fig. 2):

$$\delta\mathbf{c}_{i,j} = \begin{bmatrix} \delta c_{RXi,j} \\ \delta c_{RYi,j} \\ \delta c_{RZi,j} \\ \delta c_{TXi,j} \\ \delta c_{TYi,j} \\ \delta c_{TZi,j} \end{bmatrix} \quad \bar{\mathbf{c}}_{i,j} = \begin{bmatrix} \bar{c}_{RXYi,j} \\ \bar{c}_{RZi,j} \\ \bar{c}_{TXYi,j} \\ \bar{c}_{TZi,j} \end{bmatrix} \tag{1}$$

The *clearance constraints* for the jth axisymmetric joint of leg i can be formulated as a set of four inequalities defining a convex set:

$$(\delta c_{TXi,j})^2 + (\delta c_{TYi,j})^2 - (\bar{c}_{TXYi,j})^2 \leq 0 \tag{2}$$
$$(\delta c_{TZi,j})^2 - (\bar{c}_{TZi,j})^2 \leq 0 \tag{3}$$
$$(\delta c_{RXi,j})^2 + (\delta c_{RYi,j})^2 - (\bar{c}_{RXYi,j})^2 \leq 0 \tag{4}$$
$$(\delta c_{RZi,j})^2 - (\bar{c}_{RZi,j})^2 \leq 0 \tag{5}$$

D. Link Flexibility

The elasticity of the links is modelled by using the Virtual Joint Model (VJM) [11]. At the end of each elastic link a 6-DoF virtual elastic joint is added, while the link itself is considered rigid. The virtual elastic joint behaves as a 6-DoF spring with elastic properties similar to those of the corresponding link.

It is assumed that the virtual elastic joint coordinates have infinitesimal values, and can therefore be expressed by a 6-dimensional small displacement screw $\delta\mathbf{e}_{i,j}$ as shown in Fig. 1. To a particular value of $\delta\mathbf{e}_{i,j}$, a virtual elastic joint reaction wrench $\mathbf{w}_{Ei,j}$ and a potential energy $E_{Ei,j}$ are associated. Since the deformations of the links are assumed to be small, a linear relation exists between the virtual elastic joint reaction wrench and the virtual elastic joint coordinates, defined by a 6×6 stiffness matrix $\mathbf{K}_{Ei,j}$. $\mathbf{w}_{Ei,j}$ and $E_{Ei,j}$

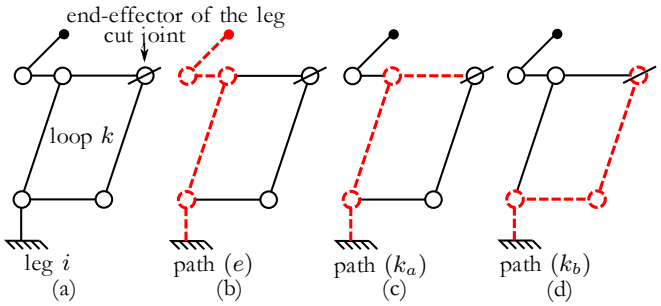

Fig. 3. (a) leg i with a closed loop and the corresponding cut joint; (b) path (in red dashed lines) to consider in order to compute the error on the ith leg end-effector pose; (c) and (d) show the two paths (in red dashed lines) to consider in order to compute the error on poses of the two cut ends of the loop.

are expressed as:

$$\mathbf{w}_{Ei,j} = \mathbf{K}_{Ei,j}\delta\mathbf{e}_{i,j} \tag{6}$$

$$E_{Ei,j} = \frac{1}{2}\delta\mathbf{e}_{i,j}{}^T\mathbf{K}_{Ei,j}\delta\mathbf{e}_{i,j} \tag{7}$$

The stiffness matrix $\mathbf{K}_{Ei,j}$ can be evaluated using FEA-based methods, considering the real geometry of the link, or analytically, by approximating the link with a simple shape. Here, all links are approximated by beams with full circular cross-section. The parameters required to compute the stiffness matrix of a link are its radius r, its Young modulus E, and its Poisson's ratio ν.

E. Joint Elasticity

To model the joint elasticity, a virtual 6-DoF elastic joint is added after the virtual joint clearance. The small displacement screw, reaction wrench, potential energy and stiffness matrix associated with the elasticity of the jth joint of leg i are denoted $\delta\mathbf{b}_{i,j}$, $\mathbf{w}_{Bi,j}$, $E_{Bi,j}$ and $\mathbf{K}_{Bi,j}$.

F. Differential Model of the Legs

Let $\delta\mathbf{x}_{i,e|0}$ be the pose error of the end-effector of leg i expressed in frame $\mathcal{F}_0$. $\delta\mathbf{x}_{i,e|0}$ is a function of $\delta\mathbf{l}_{i,j}$, $\delta\mathbf{e}_{i,j}$, $\delta\mathbf{c}_{i,j}$, $\delta\mathbf{b}_{i,j}$ and is expressed as follows:

$$\delta\mathbf{x}_{i,e|0} = \mathbf{M}_i\left(\delta\mathbf{l}_i + \delta\mathbf{c}_i + \delta\mathbf{e}_i + \delta\mathbf{b}_i\right) \tag{8}$$

$$\delta\mathbf{l}_i = \begin{bmatrix}\delta\mathbf{l}_{i,1}^T & \dots & \delta\mathbf{l}_{i,N_i}^T\end{bmatrix}^T \tag{9}$$

$$\delta\mathbf{c}_i = \begin{bmatrix}\delta\mathbf{c}_{i,1}^T & \dots & \delta\mathbf{c}_{i,N_i}^T\end{bmatrix}^T \tag{10}$$

$$\delta\mathbf{e}_i = \begin{bmatrix}\delta\mathbf{e}_{i,1}^T & \dots & \delta\mathbf{e}_{i,N_i}^T\end{bmatrix}^T \tag{11}$$

$$\delta\mathbf{b}_i = \begin{bmatrix}\delta\mathbf{b}_{i,1}^T & \dots & \delta\mathbf{b}_{i,N_i}^T\end{bmatrix}^T \tag{12}$$

$$\mathbf{M}_i = \begin{bmatrix}\mathbf{M}_{i,1} & \dots & \mathbf{M}_{i,N_i} & \prod_{k=1}^{N_i}\left(\mathbf{N}_{i,k}\right)\end{bmatrix} \tag{13}$$

$$\mathbf{M}_{i,j} = \prod_{k=1}^{N_i}\left(\mathbf{N}_{i,k}\right)\prod_{h=N_i}^{j}\left(\mathrm{adj}\left(\mathbf{T}_{i,h}\right)\right)^{-1} \tag{14}$$

$$\mathbf{N}_{i,j} = \begin{bmatrix}\mathbf{R}_{i,j} & \mathbf{0}_{3\times3}\\ \mathbf{0}_{3\times3} & \mathbf{R}_{i,j}\end{bmatrix} \tag{15}$$

where $\left(\mathrm{adj}\left(\mathbf{T}_{i,h}\right)\right)^{-1}$ is the adjoint map of $\mathbf{T}_{i,h}$.

If the ith leg of the manipulator contains closed loop(s) as shown in Fig. 3, Eq. (8) will be expressed as:

$$\delta\mathbf{x}_{i,e|0} = \mathbf{M}_i^{(e)}\left(\delta\mathbf{l}_i^{(e)} + \delta\mathbf{c}_i^{(e)} + \delta\mathbf{e}_i^{(e)} + \delta\mathbf{b}_i^{(e)}\right) \tag{16}$$

where the superscript (e) indicates that only the geometric errors and the virtual joint coordinates in the path from the base to the end-effector of leg i must be considered. Moreover, each loop is cut as described in Sec. II-A. The poses of the end-frames of the k-th loop of leg i are denoted $\mathbf{x}_{i,k_a}$ and $\mathbf{x}_{i,k_b}$, respectively. The errors on these poses are:

$$\delta\mathbf{x}_{i,k_a} = \mathbf{M}_i^{(k_a)}\left(\delta\mathbf{l}_i^{(k_a)} + \delta\mathbf{e}_i^{(k_a)} + \delta\mathbf{c}_i^{(k_a)} + \delta\mathbf{b}_i^{(k_a)}\right) \tag{17}$$

$$\delta\mathbf{x}_{i,k_b} = \mathbf{M}_i^{(k_b)}\left(\delta\mathbf{l}_i^{(k_b)} + \delta\mathbf{e}_i^{(k_b)} + \delta\mathbf{c}_i^{(k_b)} + \delta\mathbf{b}_i^{(k_b)}\right) \tag{18}$$

The superscripts (k_a) and (k_b) indicate that only the geometric errors and the virtual joint coordinates in the path from the base to the first and second cut ends of the k-th loop must be considered.

G. Assembly Constraints

In order to assemble the manipulator, the end-effectors of the legs must coincide, as well as the cut ends of every loop. It means that the errors in the pose of the corresponding frames must be equal. The following *assembly constraints* must therefore be satisfied:

$$\delta\mathbf{x}_{p|0} = \delta\mathbf{x}_{i,e|0}, i = 1\dots m \tag{19}$$

$$\delta\mathbf{x}_{i,ka} = \delta\mathbf{x}_{i,kb}, i = 1\dots m, k = 1\dots B_i \tag{20}$$

$\delta\mathbf{x}_{p|0}$ denotes the small displacement screw representing the error on the moving-platform pose in $\mathcal{F}_0$. It is composed of a rotational part $\delta\mathbf{x}_{Rp|0}$ and of a translational part $\delta\mathbf{x}_{T|0}$.

III. Computing the Assembly Zones, the Minimum Assembly Energy and the Maximum Pose Errors

This section describes the developed methodology to compute the *assembly zones*, the minimum assembly energy that is necessary to assemble the manipulator outside them, and the errors on the moving platform pose. In this section, the expression *clearance constraints* refers to the constraints (2) to (5). The expression *assembly constraints* refers to the constraints (19) and (20).

A. Computing the Assembly Zones

The following constraint satisfaction problem (CSP) is formulated in order to compute the assembly zones of parallel manipulators:

$$\begin{aligned}\text{variables } & \delta\mathbf{x}_{p|0}, \delta\mathbf{c}_{i,j}, i = 1\dots m, j = 1\dots N_i\\ \text{constraints } & \text{clearance constraints}\\ & \text{assembly constraints}\end{aligned} \tag{21}$$

The constraints form a convex set. Therefore, problem (21) can be solved by convex programming techniques [14].

In the formulation of the assembly constraints only the small displacement screws related to geometric errors $\delta\mathbf{l}_{i,j}$ and joint clearances $\delta\mathbf{c}_{i,j}$ are considered. Solving this problem allows to determine whether it is possible, in a given

configuration, to assemble the manipulator by exploiting joint clearances only. This is equivalent to say that the manipulator can be assembled without deforming its links and joints and, therefore, without introducing any internal stress.

B. Computing the Minimum Assembly Energy

The following optimization problem is formulated in order to compute the minimum assembly energy:

$$\begin{aligned} \text{minimize } & E = \sum_{i=1}^{m} \sum_{j=1}^{N_i} (E_{Ei,j} + E_{Bi,j}) \\ \text{over } & \delta\mathbf{x}_{p|0}, \delta\mathbf{c}_{i,j}, \delta\mathbf{e}_{i,j}, \delta\mathbf{b}_{i,j}, i = 1 \dots m, j = 1 \dots N_i \\ \text{subject to } & \text{clearance constraints} \\ & \text{assembly constraints} \end{aligned} \tag{22}$$

The objective function of problem (22) is the elastic potential energy of the manipulator. Its minimization makes sense from a physical point of view, since in theory the manipulator should be naturally assembled in a configuration in which the elastic potential energy is a minimum. The objective to be minimized is a convex quadratic function. The constraints of the optimization problem at hand form a convex set. The minimum energy problem is therefore in the most general case a convex second order-cone programming (SOCP) that can be solved by convex optimization techniques [14].

Inside the assembly zones this problem finds a minimum equal to zero, since there is no need to deform links and joints. Outside the assembly zones the limits of the joint clearances are reached, and therefore it is necessary to deform links and joints to assemble the manipulator and the minimum energy required to assemble the parallel manipulator is not null.

C. Elastic Reaction Wrench on the Moving-platform

If the legs of the manipulator are simple serial chains, the elastic reaction wrench on the end-effector of leg i, $\mathbf{w}_{i,e}$, can be computed with the following expression [11]:

$$\mathbf{w}_{i,e} = \mathbf{w}_{Ei,e} + \mathbf{w}_{Bi,e} \tag{23}$$

$$\mathbf{w}_{Ei,e} = \left(\mathbf{M}_i \mathbf{K}_{Ei}^{-1} \mathbf{M}_i^T\right)^{-1} \mathbf{M}_i \delta\mathbf{e}_i \tag{24}$$

$$\mathbf{w}_{Bi,e} = \left(\mathbf{M}_i \mathbf{K}_{Bi}^{-1} \mathbf{M}_i^T\right)^{-1} \mathbf{M}_i \delta\mathbf{b}_i \tag{25}$$

$\mathbf{w}_{Ei,e}$ and $\mathbf{w}_{Bi,e}$ are the reaction wrenches associated to the link and joint deformations, respectively. The values of the screws $\delta\mathbf{e}_i$ and $\delta\mathbf{b}_i$ are found by solving problem (22).

Once the reaction wrenches applied on the end-effectors of the single legs are known, the total reaction wrench applied on the moving-platform, denoted $\mathbf{w}_p$, is computed by summing them, since the end-effectors are coincident:

$$\mathbf{w}_p = \begin{bmatrix} \mathbf{m}_p \\ \mathbf{f}_p \end{bmatrix} = \sum_{i=1}^{m} \mathbf{w}_{i,e} \tag{26}$$

where $\mathbf{m}_p$ and $\mathbf{f}_p$ are the reaction force and moment applied at the geometric center of the moving-platform, respectively.

In the case the parallel manipulator has parallelogram joints, the latter can be replaced by single links having equivalent elastic properties as explained in [13].

D. Computing the Maximum Pose Error

Two distinct problems are formulated, one to find the maximum orientation error and one to find the maximum position error of the moving platform:

$$\begin{aligned} \text{minimize } & -r^2 = -\delta\mathbf{x}_{Rp|0}^T \delta\mathbf{x}_{Rp|0}, \text{ or} \\ & -t^2 = -\delta\mathbf{x}_{Tp|0}^T \delta\mathbf{x}_{Tp|0} \\ \text{over } & \delta\mathbf{x}_{p|0}, \delta\mathbf{c}_{i,j}, i = 1 \dots m, j = 1 \dots N_i \\ \text{subject to } & \text{clearance constraints} \\ & \text{assembly constraints} \end{aligned} \tag{27}$$

The objective function is the opposite of the square of the orientation error r or of the position error t of the moving-platform expressed in frame $\mathcal{F}_0$. The link flexibilities $\delta\mathbf{e}_{i,j}$ and joint elasticities $\delta\mathbf{b}_{i,j}$ are not part of the decision variables. However, they appear in the expressions of the assembly constraints. Their values are taken from the solution of the minimum assembly energy problem (22). This allows us to determine the maximum pose error of the moving-platform in every point of the manipulator workspace, even outside the assembly zones that are defined assuming that the links and joints are rigid.

The objective to be minimized is a concave quadratic function, while the constraints form a convex set. The maximum error problems is therefore a nonconvex quadratically constrained quadratic programs (QCQPs). To solve them, special techniques are required. Here, a branch and bound algorithm is used [15]. The branch and bound algorithm does not provide a single value as a result, but two values that bound the real error from below and above. It is possible to arbitrarily choose the tolerance ϵ representing the maximum distance between these bounds.

IV. Case Study: IRSbot-2

A. Description of the IRSbot-2

The IRSbot-2 (IRCCyN Spatial Robot with 2 Degrees of Freedom) is a parallel manipulator designed for fast and accurate pick and place operations in a two-dimensional workspace [16]. The IRSbot-2 shown in Fig. 4 is expected to reach an acceleration up to 20 G and an accuracy equal to 20 μm throughout a parallelepiped of 800 mm side length.

The base and the moving-platform are connected by two legs. Each leg is composed of a *proximal* module and a *distal* module mounted in series. The proximal module is a parallelogram, made up of four revolute joints of axes perpendicular to the $(\mathbf{x}_0, \mathbf{z}_0)$ plane. One of the link is fixed with respect to the base frame $\mathcal{F}_0$, allowing the opposite link, connected to the elbow, to have a constant orientation with respect to it. The distal module is made up of two links connected to the elbow and to the base by universal joints. The universal joints can be represented by two revolute joints whose axes are perpendicular to each other and intersect. The axes of both joints are perpendicular to the link they are connected to. Some of these joints are compliant, and have no clearance but can be deformed elastically. Four planes, parallel to each other, are defined (see Fig. 4): a *base plane* $\mathcal{P}_0$, a *platform plane* $\mathcal{P}_p$, and two *elbow planes* $\mathcal{P}_1$ and $\mathcal{P}_2$.

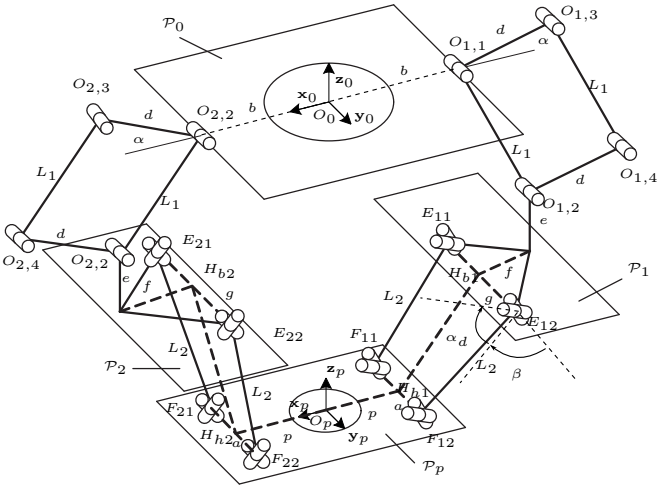

Fig. 4. Parameterization of the IRSbot-2.

The IRSBot-2 has two legs ($m = 2$), each with twelve joints ($n_1 = n_2 = 12$) and two loops ($B_1 = B_2 = 2$). Four additional frames are added to each leg of the manipulator in order to simplify its parametrization. In total, $N_i = 21$ frames are defined for each leg. The geometric parameters that are necessary to completely define the architecture of a leg are defined as follows (Fig. 4):

- b is the distance between the first joint of the parallelogram and the origin of the base frame.
- d is the length of the fixed side of the parallelogram.
- L_1 is the length of the moving side of the parallelogram.
- $\begin{bmatrix} f & g & e \end{bmatrix}^T$ is the vector describing the position of the universal joints with respect to the ends of the parallelogram joints, expressed in the base frame.
- L_2 is the length of the links of the distal module.
- $\begin{bmatrix} p & a & 0 \end{bmatrix}^T$ is the vector describing the position of the platform with respect to the last universal joints of the links of the distal module, expressed in the base frame.
- α is the angle between the platform plane and the link of the parallelogram that is fixed to the base.
- β and α_d are the azimuth and altitude angles that describe the orientation of the second revolute joint of each universal joint with respect to the first one.

The nominal geometric parameters of the IRSbot2 are the following: $a = 50$ mm; $b = 83$ mm; $d = 106$ mm; $e = 3.342$ mm; $f = 80$ mm; $g = 166$ mm; $p = 50$ mm; $L_1 = 321$ mm; $L_2 = 452$ mm; $\alpha = \frac{\pi}{6}$ rad; $\alpha_d = \frac{\pi}{4}$ rad; $\beta = \frac{\pi}{2}$ rad.

In the scope of this paper, the proximal modules are considered perfect in order to reduce the computational times. Therefore, all screws $\delta\mathbf{l}_{i,j}$, $\delta\mathbf{c}_{i,j}$, $\delta\mathbf{e}_{i,j}$, and $\delta\mathbf{b}_{i,j}$ are null for $j = 1 \ldots 4$.

The screws $\delta\mathbf{l}_{i,j}$ are null for $j \neq 5, 8, 11, 14, 19, 21$ (these frames were added to simplify the robot modeling or do not correspond to real links). The values of the remaining geometric error screws are selected randomly between $\underline{\delta\mathbf{l}}$ and $\overline{\delta\mathbf{l}}$, defined as follows:

$$\underline{\delta\mathbf{l}} = \begin{bmatrix} 10^{-4} \text{ rad} \\ 10^{-4} \text{ rad} \\ 10^{-4} \text{ rad} \\ 10^{-3} \text{ mm} \\ 10^{-3} \text{ mm} \\ 10^{-3} \text{ mm} \end{bmatrix} \quad \overline{\delta\mathbf{l}} = \begin{bmatrix} 2 \cdot 10^{-2} \text{ rad} \\ 2 \cdot 10^{-2} \text{ rad} \\ 2 \cdot 10^{-2} \text{ rad} \\ 2 \cdot 10^{-1} \text{ mm} \\ 2 \cdot 10^{-1} \text{ mm} \\ 2 \cdot 10^{-1} \text{ mm} \end{bmatrix}$$

All joints are considered axi-symmetric for the determination of the clearance constraints. The screws $\delta\mathbf{c}_{i,j}$ are null for $j \neq 7, 8, 13, 14$. These frames are not associated to a joint or are associated to a compliant joint without clearance. The other joint clearance constraints are defined by Eq. (1) with vectors $\overline{\mathbf{c}}_{i,j}$ taking the following values:

$$\overline{\mathbf{c}}_{i,j} = \begin{bmatrix} 7.55 \cdot 10^{-4} \text{ rad} \\ 10 \text{ rad} \\ 29 \cdot 10^{-3} \text{ mm} \\ 29 \cdot 10^{-3} \text{ mm} \end{bmatrix}$$

The screws $\delta\mathbf{e}_{i,j}$ are null for $j \neq 8, 14$. Only the two long links of the distal modules are assumed to be flexible. The Young modulus is set as $E = 6 \cdot 10^{10}$ Pa, the Poisson's ratio as $\nu = 0.3$, and the radius of the links as $r = 40$ mm.

The screws $\delta\mathbf{b}_{i,j}$ are null for $j \neq 6, 9, 12, 15$, as these joints are not compliant. For the other joints the stiffness matrix is defined as follows, according to the technical data of the employed compliant joints:

$$\mathbf{K}_B = \text{diag}\left(10^8 \text{ Nm}, 10^8 \text{ Nm}, 1 \text{ Nm}, 3.51 \times 10^8 \text{ N/m}, 3.51 \times 10^8 \text{ N/m}, 4.39 \times 10^8 \text{ N/m}\right)$$

The optimization problems defined in Sec. III are solved over the full half-workspace for $y \leq 0$, on points sampled with a step of 25 mm along both the $\mathbf{x}_0$ and $\mathbf{z}_0$ axes. The tolerance for the branch and bound algorithm is set to $\epsilon = 10^{-6}$ rad for the orientation errors and to $\epsilon = 10^{-3}$ mm for the position errors.

B. Results

Figure 5 shows the assembly zones, the minimum assembly energy and the upper bounds of the maximum orientation and position errors of the moving-platform for the IRSbot-2. The error plots are given for both the complete case and for a case where only joint clearances are considered (the screws $\delta\mathbf{l}_{i,j}$, $\delta\mathbf{e}_{i,j}$, and $\delta\mathbf{b}_{i,j}$ are all set to zero).

For the chosen geometric errors, assembling the manipulator presents many difficulties in many areas of the workspace. The minimum assembly energy is high throughout the whole manipulator workspace, and the components of the wrench associated to the maximum assembly energy point have very large values. In such a case, the manipulator cannot be assembled. Therefore, the dimensional tolerances of the geometric parameters for the real robot should be lower than those selected for this simulation.

When all screws are considered, the error is relatively high, and its distribution does not present any regularity. When only joint clearances are considered, the error has instead a regular and symmetric distribution and reaches lower values.

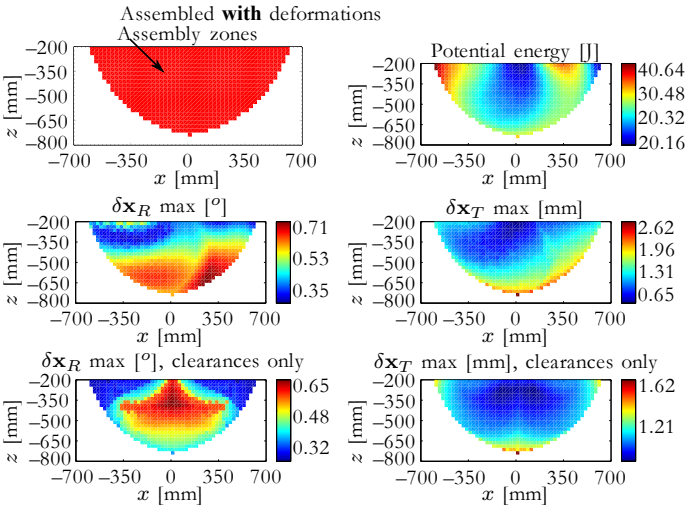

Fig. 5. Assembly zones (top-left). Minimum assembly energy (top-right). Upper bounds of the maximum orientation errors (centre-left) and of the maximum position errors (centre-right) of the moving-platform, while considering geometric errors, joint clearances and link flexibilities. Upper bounds of the maximum orientation errors (bottom-left) and of the maximum position errors (bottom-right) of the moving-platform, while considering joint clearances only.

The contribution to the pose error of the clearance displacements usually has a symmetric distribution, because clearance boundaries are symmetric and equal for all joints from one leg to the other one. On the contrary, the contribution to the pose error of the geometric errors is irregular throughout the manipulator workspace because the small displacement screws associated to the geometric errors differ for every frame in the manipulator. Here, the order of magnitude of the geometric errors is larger than the order of magnitude of the clearance boundaries. Therefore, the regular contribution of the clearance displacements is negligible and is masked by the more relevant and irregular contributions of the geometric errors.

V. Conclusions and Future Work

A method to determine the assembly energy, the internal elastic reaction wrenches and the maximum pose error of parallel manipulators subject to geometric errors, joint clearances, link flexibility and joint elasticity has been developed and applied to a two-dof spatial parallel manipulator, named IRSbot-2.

It has been shown that outside the assembly zones, as expected, links are bent and the assembly energy increases smoothly. The maximum error on the moving-platform pose has different contributions due to geometric errors, clearances and flexibilities. The pose error due to joint clearances has a regular and symmetric distribution throughout the manipulator workspace, due to the symmetry of the clearance bounds and of the legs. The pose error due to geometric errors and elasticity displacements, on the contrary, is highly irregular due to the asymmetry of the geometric errors from one leg to the other one.

This research work opens the way to many further developments. First of all, the proposed method can be applied to other manipulators and used to analyse the kinematic behaviour of the manipulators close to their parallel singularities. Secondly, the error on the moving-platform pose can be studied statistically in order to determine the most probable error instead of the worst-case error. The method lacks experimental validations due to the difficulty of taking the necessary measurements on real manipulators. An experimental validation will prove that the results provided by the developed method are realistic and reliable. Finally, it would be relevant to relate the assembly energy to the stress in the links in order to verify that the links do not break with their deformations required for the assembly of the parallel manipulator.

Acknowledgment

The authors would like to acknowledge the financial support of the ANR, France (Project ANR-2011-BS3-006-01-ARROW).

References

[1] N. Binaud, P. Cardou, S. Caro, P. Wenger, The kinematic sensitivity of robotic manipulators to joint clearance, Proceedings of ASME Design Engineering Technical Conferences, 2010

[2] C. Han, J. Kim, J. Kim, F. C. Park, Kinematic sensitivity analysis of the 3-UPU parallel mechanism, vol. 37, no. 8, pp. 787-798, 2002

[3] V. P. Castelli, S. Venanzi, Kinetostatic modeling of the clearance-affected prismatic pair, Journal of Robotic Systems, vol. 22, no. 9, pp 487-496, 2001

[4] V. P. Castelli, S. Venanzi, Recent techniques for clearance influence analysis in planar and spatial mechanisms, Rendiconti - Istituto Lombardo. Accademia di Scienza e di Leggere. Scienze matematiche e applicazioni, vol. 138, pp. 1-14, 2004

[5] H. H. S. Wang, B. Roth, Position errors due to clearance in journal bearings, Journal of Mechanisms, Transmissions, and Automation in Design, vol. 111, no. 3, pp. 315-320, 2001

[6] P. Flores, J. Ambrósio, J. C. P. Claro, H. M. Lankarani, Dynamic behaviour of planar rigid multi-body systems including revolute joints with clearance, Proceedings of the Institution of Mechanical Engineers, Part K: Journal of Multi-body Dynamics, vol. 221, no. 2, pp. 161-174, 2007

[7] P. Flores, Modeling and simulation of wear in revolute clearance joints in multibody systems, Mechanism and Machine Theory, vol. 44, no. 6, pp. 1211-1222, 2009

[8] C. M. Gosselin, Stiffness analysis of parallel mechanisms using a lumped model, International Journal of Robotics and Automation, vol. 17, pp. 17-27, 2002

[9] J. K. Salisbury, Active stiffness control of a manipulator in Cartesian coordinates, Decision and Control including the Symposium on Adaptive Processes, vol. 19, pp. 95-100, 1980

[10] Non-linear joint dynamics and control of jointed flexible structures with active and visco-elastic joint actuators, Journal of Sound and Vibration, vol. 143, no. 3, pp. 407-422, 1990

[11] A. Pashkevich, D. Chablat, P. Wenger, Stiffness analysis of overconstrained parallel manipulators, Mechanism and Machine Theory, vol. 44, no. 5, pp. 966-982, 2008

[12] A. Pashkevich, A. Klimchick, S. Caro, D. Chablat, Stiffness analysis of parallel manipulators under auxiliary loadings, The ASME 2012 International Design Engineering Technical Conferences (IDETC) and Computers and Information in Engineering Conference (CIE), 2010

[13] A. Pashkevich, A. Klimchik, S. Caro, D. Chablat, Stiffness modelling of parallelogram-based parallel manipulators, New Trends in Mechanism Science, pp. 675-682, 2010

[14] S. Boyd, L. Vandenberghe (2004). Convex Optimization (pdf). Cambridge University, Press. ISBN 978-0-521-83378-3

[15] R. E. Moore (1966). Interval Analysis. Englewood Cliff, New Jersey: Prentice-Hall.

[16] C. Germain, S. Caro, S. Briot, P. Wenger, Singularity-free Design of the Translational Parallel Manipulator IRSBot-2, Mechanism and Machine Theory, Vol. 64, pp. 262–285, 2013.